Available online at www.sciencedirect.com
ScienceDirect
Journal of Sound and Vibration 310 (2008) 197–216
JOURNAL OF SOUND AND VIBRATION
www.elsevier.com/locate/jsvi

Analysis of solid elastic cylinders with internal losses using complete sets of functions

D.D. Ebenezer[a,*], K. Nirnimesh[b], Rahul Barman[b], Rajnish Kumar[b], Shashi Bhushan Singh[b]

[a]*Naval Physical and Oceanographic Laboratory, Thrikkakara, Kochi 682 021, India*
[b]*Department of Ocean Engineering and Naval Architecture, Indian Institute of Technology, Kharagpur, India*

Received 7 February 2007; received in revised form 5 June 2007; accepted 28 July 2007
Available online 3 October 2007

Abstract

A method to determine the response of a solid, elastic, isotropic cylinder with internal losses and arbitrary length to radius ratio to excitations acting on its surface is presented. The method is based on the use of complete sets of functions and the response to arbitrary excitations can be analysed. It is illustrated for axisymmetric excitations that are anti-symmetric with respect to the plane midway between the ends of the cylinder. Excitations that are symmetric have been considered earlier. [D.D. Ebenezer et al., Forced vibrations of solid elastic cylinders, *Journal of Sound and Vibration* 282 (2005) 991–1007]. All components of displacement and stress are expressed as a sum of two infinite series that contain terms that are complete in the axial and radial direction, respectively. Therefore, arbitrary boundary conditions can be satisfied. In lossless cylinders, for each chosen set, there are difficulties at those frequencies at which certain functions become zero. Some other complete set of functions can be used at these frequencies. However, this difficulty does not arise for cylinders with losses. Two different sets are used to compute the resonance frequencies of lossless cylinders. The responses of cylinders with internal losses to uniform and concentrated excitations on the flat and curved surfaces are also presented to illustrate the approach. They are in good agreement with results obtained using ATILA—a finite element software package.

1. Introduction

Complete sets of functions have been recently [1–3] used to analyse forced vibrations of solid elastic and piezoelectric cylinders. This is possible because arbitrary functions can be expressed as weighted sums of the functions. In general, more than one complete set can be used to obtain the same result. A well-known example is the expansion using Fourier cosine and Fourier sine series after assuming that the function is symmetric and anti-symmetric, respectively. In this paper, two different complete sets of functions are used to analyse solid elastic cylinders and the same results are obtained. The forced vibrations of cylinders with internal losses represented by complex material properties are also analysed using complete sets.

*Corresponding author. Tel.: +91 484 242 2598; fax: +91 484 242 4858.
E-mail address: tsonpol@vsnl.com (D.D. Ebenezer).

0022-460X/$ - see front matter © 2007 Elsevier Ltd. All rights reserved.
doi:10.1016/j.jsv.2007.07.050

A review of the literature on finite elastic cylinders was presented by Ebenezer et al. [2]. Earlier, Soldatos [4] presented a comprehensive review of the literature on finite and infinite cylinders. There is considerable interest in the analysis of cylinders because they are used in a variety of engineering applications including electroacoustic transducers [5,6]. The classical Langevin transducer consists of one or more piezoelectric cylinders sandwiched between two elastic cylinders. Iula [7] and Shuyu [8] have analysed this type of transducer using approximate models of cylinders. 1-3 piezocomposite transducers [9] consist of piezoelectric rods embedded in a lossy elastic matrix and are widely used as underwater broadband transmitters and receivers. They can be analysed using models of a solid piezoelectric cylinder and a hollow elastic cylinder.

In transducer applications, the excitation on the cylinders is seldom purely symmetric or purely anti-symmetric with respect to the plane midway between the ends of the cylinder. Therefore, it is necessary to develop methods that can be used to determine the response to general excitations, i.e., the sum of symmetric and anti-symmetric components. A method to determine the response to excitations that are symmetric has been presented in Ref. [2]. In this paper, a method is presented to determine the response to anti-symmetric excitations.

The work presented here is a continuation of the work reported in Refs. [1–3] and is based on the method used by Hutchinson [10] to analyse the free vibration of cylinders. Weighted sums of only certain exact solutions to the equations of motion are used to determine the response to axisymmetric excitations. One infinite set of solutions is chosen such that each field variable is expressed in terms of Bessel functions that form a complete set in the radial direction. Another infinite set of solutions is chosen such that each field variable is expressed in terms of trigonometric functions that form a complete set in the axial direction. Each term in both the series is an exact solution to the exact equations of motion. A double sum is necessary when the excitation is non-axisymmetric. In principle, any complete set of functions can be used. This is illustrated here by using two different complete sets of functions in the axial direction.

Structures have internal losses and heat is generated when they vibrate. Losses are modelled here using complex material properties and the analysis is therefore valid only for steady-state vibrations. Holland [11] derived the conditions satisfied by the imaginary parts of the 10 coefficients that are required to completely describe piezoelectric ceramics. The conditions were derived by constraining the structure to dissipate energy and not create it when it vibrates. Similar conditions for isotropic elastic materials are derived here by using the conditions derived by Holland.

Numerical results are presented for free as well as forced vibrations and are in excellent agreement with those obtained using ATILA [12]—a commercial finite element package. The difference between the resonance frequencies computed using the present method and ATILA is in the sixth significant digit in most cases. The displacements of cylinders with loss excited by distributed forces are also in very good agreement with finite element results.

2. Theory

Consider a solid, elastic, isotropic cylinder of finite length L and radius a with internal losses as shown in Fig. 1. Non-uniform, axisymmetric, stresses or displacements are specified on the surfaces of the cylinder. The response of the cylinder is of interest.

The excitation and, therefore, the response of the cylinder are axisymmetric. The dynamic equilibrium equations are expressed in cylindrical coordinates (r, θ, z) as [13,14]

$$\frac{\partial T_{rz}}{\partial r}+\frac{1}{r}T_{rz}+\frac{\partial T_{zz}}{\partial z}=-\rho\omega^2 U \tag{1a}$$

and

$$\frac{\partial T_{rr}}{\partial r}+\frac{\partial T_{rz}}{\partial z}+\frac{1}{r}(T_{rr}-T_{\theta\theta})=-\rho\omega^2 W, \tag{1b}$$

where U and W are the axial and radial displacements, respectively, T_{rr}, $T_{\theta\theta}$, T_{zz}, and T_{rz} are components of stress, ρ is the density, and ω is the angular frequency. The components of strain are

$$[S_{rr},\ S_{\theta\theta},\ S_{zz},\ S_{rz}]=\left[\frac{\partial W}{\partial r},\ \frac{W}{r},\ \frac{\partial U}{\partial z},\ \frac{\partial U}{\partial r}+\frac{\partial W}{\partial z}\right]. \tag{2}$$

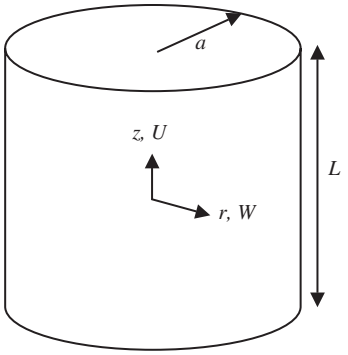

Fig. 1. A solid cylinder of length L and radius a. The axial and radial components of displacement are U and W, respectively.

The constitutive relations for an isotropic elastic cylinder are

$$\begin{Bmatrix} T_{rr} \\ T_{\theta\theta} \\ T_{zz} \\ T_{rz} \end{Bmatrix} = \begin{bmatrix} \lambda+2\mu & \lambda & \lambda & 0 \\ \lambda & \lambda+2\mu & \lambda & 0 \\ \lambda & \lambda & \lambda+2\mu & 0 \\ 0 & 0 & 0 & \mu \end{bmatrix} \begin{Bmatrix} S_{rr} \\ S_{\theta\theta} \\ S_{zz} \\ S_{rz} \end{Bmatrix}, \tag{3}$$

where the Lame's constants λ and μ are complex because of internal losses.

The exact axisymmetric governing equations are obtained by substituting Eqs. (2) and (3) in Eq. (1) and expressed as

$$\begin{bmatrix} (\lambda+2\mu)\dfrac{\partial^2}{\partial z^2}+\mu\left[\dfrac{\partial^2}{\partial r^2}+\dfrac{1}{r}\dfrac{\partial}{\partial r}\right]+\rho\omega^2 & (\lambda+\mu)\left[\dfrac{\partial^2}{\partial r\partial z}+\dfrac{1}{r}\dfrac{\partial}{\partial z}\right] \\ (\lambda+\mu)\dfrac{\partial^2}{\partial r\partial z} & (\lambda+2\mu)\left[\dfrac{\partial^2}{\partial r^2}+\dfrac{1}{r}\dfrac{\partial}{\partial r}-\dfrac{1}{r^2}\right]+\mu\dfrac{\partial^2}{\partial z^2}+\rho\omega^2 \end{bmatrix} \begin{Bmatrix} U \\ W \end{Bmatrix} = \begin{Bmatrix} 0 \\ 0 \end{Bmatrix}. \tag{4}$$

It is easily verified that

$$[U \;\; W]^{\mathrm{T}} = [U_1 \;\; W_1]^{\mathrm{T}} + [U_2 \;\; W_2]^{\mathrm{T}} \tag{5a}$$

is the sum of two exact solutions to Eq. (4) where

$$\begin{Bmatrix} U_1 \\ W_1 \end{Bmatrix} = \begin{Bmatrix} P\cos(K_1 z) \\ 0 \end{Bmatrix} + \begin{Bmatrix} \sum_{m=1}^{M_r}\sum_{s=1}^{2} P_{ms}J_0(k_{rm}r)\cos(k_{zms}z) \\ \sum_{m=1}^{M_r}\sum_{s=1}^{2} P_{ms}\psi_{ms}J_1(k_{rm}r)\sin(k_{zms}z) \end{Bmatrix}, \tag{5b}$$

$$\begin{Bmatrix} U_2 \\ W_2 \end{Bmatrix} = \begin{Bmatrix} QJ_0(K_2 r) \\ 0 \end{Bmatrix} + \begin{Bmatrix} \sum_{m=1}^{M_z}\sum_{s=1}^{2} Q_{ms}J_0(k_{rms}r)\cos(k_{zm}z) \\ \sum_{m=1}^{M_z}\sum_{s=1}^{2} Q_{ms}\chi_{ms}J_1(k_{rms}r)\sin(k_{zm}z) \end{Bmatrix}, \tag{5c}$$

$$K_s = \omega/c_s, \quad s = 1, 2, \tag{5d}$$

$$c_1^2 = \frac{\lambda+2\mu}{\rho}, \quad c_2^2 = \frac{\mu}{\rho} \tag{5e}$$

and J_v is the vth-order Bessel function of the first kind. P, Q, P_{ms}, and Q_{ms} are weights that depend on the excitation. Eqs. (5b) and (5c) are exact solutions for arbitrary values of k_{rm}, $m = 1, 2, 3, \ldots, M_r$ and k_{zm}, $m = 1, 2, 3, \ldots, M_z$.

The frequency-dependent values of k_{zms} are determined by substituting Eq. (5b) in Eq. (4) and equating the determinant of the resulting equation to zero. The characteristic equation is quadratic in ${k_{zms}}^2$ and is solved for $m = 1, 2, \ldots, M_r$ to obtain

$$k_{zms} = \sqrt{K_s^2 - k_{rm}^2}, \quad s = 1, 2. \tag{6}$$

Similarly, the frequency-dependent values of k_{rms} are determined by substituting Eq. (5c) in Eq. (4) and equating the determinant of the resulting equation to zero. The characteristic equation is quadratic in k_{rms}^2 and is solved for $m = 1, 2 \ldots, M_z$ to obtain

$$k_{\mathrm{rms}} = \sqrt{K_s^2 - k_{zm}^2}, \quad s = 1, 2, \tag{7}$$

ψ_{ms} and χ_{ms} are then obtained by substituting Eqs. (5b) and (5c), respectively, in Eq. (4) and rearranging. They are expressed as

$$\psi_{m1} = -\frac{k_{rm}}{k_{zm1}}, \quad \psi_{m2} = \frac{k_{zm2}}{k_{rm}} \tag{8a,b}$$

and

$$\chi_{m1} = -\frac{k_{zm}}{k_{rm1}}, \quad \chi_{m2} = \frac{k_{rm2}}{k_{zm}}, \tag{8c,d}$$

respectively.

Other quantities of interest are now easily determined by using Eqs. (2), (3), and (5). The components of stress are expressed as

$$\begin{aligned} T_{rr} = & -P[K_1\lambda \sin(K_1 z)] \\ & + \sum_{m=1}^{M_z}\sum_{s=1}^{2} P_{ms}\left\{\left[(\lambda+2\mu)\psi_{ms}k_{rm} - \lambda k_{zms}\right]J_0(k_{rm}r) - \frac{2\mu}{r}\psi_{ms}J_1(k_{rm}r)\right\}\sin(k_{zms}z) \\ & + \sum_{m=1}^{M_z}\sum_{s=1}^{2} Q_{ms}\left\{\left[(\lambda+2\mu)\chi_{ms}k_{rms} - \lambda k_{zm}\right]J_0(k_{rms}r) - \frac{2\mu}{r}\chi_{ms}J_1(k_{rms}r)\right\}\sin(k_{zm}z), \end{aligned} \tag{9}$$

$$\begin{aligned} T_{zz} = & -P[(\lambda+2\mu)K_1 \sin(K_1 z)] \\ & + \sum_{m=1}^{M_r}\sum_{s=1}^{2} P_{ms}J_0(k_{rm}r)\left[-(\lambda+2\mu)k_{zms} + \lambda\psi_{ms}k_{rm}\right]\sin(k_{zms}z) \\ & + \sum_{m=1}^{M_z}\sum_{s=1}^{2} Q_{ms}J_0(k_{rms}r)\left[-(\lambda+2\mu)k_{zm} + \lambda\chi_{ms}k_{rms}\right]\sin(k_{zm}z) \end{aligned} \tag{10}$$

and

$$\begin{aligned} T_{rz} = & -Q[\mu K_2 J_1(K_2 r)] \\ & + \mu\sum_{m=1}^{M_r}\sum_{s=1}^{2} P_{ms}J_1(k_{rm}r)\left[-k_{rm} + \psi_{ms}k_{zms}\right]\cos(k_{zms}z) \\ & + \mu\sum_{m=1}^{M_z}\sum_{s=1}^{2} Q_{ms}J_1(k_{rms}r)\left[-k_{rms} + \chi_{ms}k_{zm}\right]\cos(k_{zm}z). \end{aligned} \tag{11}$$

The expressions for displacement and stress are used to satisfy arbitrary boundary conditions on the surfaces by choosing the values of $k_{rm}a$ and $k_{zm}L/2$ such that all field variables are expressed in terms of complete sets in the axial and radial directions. In this paper, $k_{rm}a$ are chosen [2,10] to be the roots of

$J_1(k_{rm}a) = 0$ and are approximately equal to 0, 3.83, 7.02, 10.17,... for $m = 0, 1, 2, 3, \ldots$, respectively. In the leading term in Eq. (5b) that corresponds to $m = 0$, $k_{rm}a$ and radial displacement are zero but axial displacement is non-zero and a function of $K_1 z$. It is noted that for $M_r = \infty$, $J_v(k_{rm}r)$ form a point-wise complete set of functions when $v = 0$ and a norm-wise complete set of functions when $v = 1$. (Sets of functions that are not all zero at the same point and form a norm-wise complete sets of functions are known as point-wise complete sets.) Each term in the sets is orthogonal to the other terms, i.e., [15]

$$\int_0^a J_v(k_{rm}r)J_v(k_{rn}r)r\,\mathrm{d}r = \begin{cases} \delta_{vm}\delta_{mn}\dfrac{a^2}{2}, & m = 0, \\ \delta_{mn}\dfrac{a^2}{2}J_0^2(k_{rm}a), & m = 1, 2, \ldots \end{cases} \qquad v = 0 \quad \text{or} \quad 1, \tag{12}$$

where the Kroneker delta, δ_{mn}, is one when $m = n$ and zero otherwise.

In this paper, the cylinder is analysed using two different sets of functions that are complete in the axial direction. In the first set, k_{zm} are chosen such that

$$k_{zm}L/2 = (2m - 1)\pi/2, \quad m = 1, 2, 3, \ldots M_z, \tag{13}$$

where M_z is ∞. The series begins with the $m = 1$ term, the $\cos(.)$ terms form a complete set, and Q in Eq. (5c) is set to zero as the term is not necessary. In the second set, k_{zm} are chosen such that

$$k_{zm}L/2 = m\pi, \quad m = 0, 1, 2, 3, \ldots, M_z. \tag{14}$$

Here, the series begins with the $m = 0$ term. In the first term, W is zero but U is a function of $K_1 z$ and the term containing Q in Eq. (5c) is the first term in the series. In both sets, for $M_z = \infty$, $\sin(k_{zm}z)$ and $\cos(k_{zm}z)$ are complete sets of functions that are orthogonal, i.e.,

$$\int_{-L/2}^{+L/2} \sin(k_{zm}z)\sin(k_{zn}z)\,\mathrm{d}z = \delta_{mn}L/2 \tag{15a}$$

and

$$\int_{-L/2}^{+L/2} \cos(k_{zm}z)\cos(k_{zn}z)\,\mathrm{d}z = \begin{cases} 0, & m \neq n, \\ L/2, & m = n \neq 0, \\ L, & m = n = 0. \end{cases} \tag{15b}$$

In Eq. (5), the axial displacement is symmetric and the radial displacement is anti-symmetric about the plane midway between the ends of the cylinder. Axial and radial displacements that are anti-symmetric and symmetric, respectively, are considered in Ref. [2]. In the general case, U and W are expressed as the sum of the symmetric and anti-symmetric terms.

It is seen from the above that all field variables are expressed in terms of over-complete sets of functions. (An over-complete set of functions is the sum a point-wise or norm-wise complete set of functions and other functions.) On the flat, electroded surfaces, U, and T_{zz} are expressed in terms of $J_0(k_{rm}r)$, $m = 0, 1, 2, \ldots$, and W and T_{rz} are expressed in terms of $J_1(k_{rm}r)$, $m = 1, 2, \ldots$. On the curved surfaces, U and T_{rz} are expressed in terms of $\cos(K_{zm}z)$; and W and T_{rr} are expressed in terms of $\sin(K_{zm}z)$. It therefore follows that arbitrary, piecewise continuous, and localised boundary conditions and continuity conditions can be satisfied.

However, for lossless cylinders, when $\omega = k_{rn}c_s$ and $k_{zn}c_s$, $n = 1, 2, 3, \ldots$, $s = 1, 2$, it is seen from Eqs. (6) and (7) that the values of k_{zns} and k_{rns}, respectively, are zero, and the form of the solution in Eq. (5) is not valid at these frequencies. Therefore, the term

$$\begin{Bmatrix} U_1 \\ W_1 \end{Bmatrix} = \begin{Bmatrix} \sum_{s=1}^{2} P_{ns}J_0(k_{rn}r)\cos(k_{zns}z) \\ \sum_{s=1}^{2} P_{ns}\psi_{ns}J_1(k_{rn}r)\sin(k_{zns}z) \end{Bmatrix}$$

in Eq. (5b) is replaced by

$$\left\{ \begin{array}{l} U_1 \\ W_1 \end{array} \right\} = \left\{ \begin{array}{l} P_{n1} \cos(K_1 z) \\ 0 \end{array} \right\} + \left\{ \begin{array}{l} 0 \\ P_{n2} J_1(K_1 r) \end{array} \right\} \tag{16a}$$

at $\omega = k_{rn} c_1$ and by

$$\left\{ \begin{array}{l} U_1 \\ W_1 \end{array} \right\} = \left\{ \begin{array}{l} P_{n1} J_0(K_2 r) \\ 0 \end{array} \right\} + \left\{ \begin{array}{l} 0 \\ P_{n2} \sin(K_2 z) \end{array} \right\} \tag{16b}$$

at $\omega = k_{rn} c_2$. Similarly,

$$\left\{ \begin{array}{l} U_2 \\ W_2 \end{array} \right\} = \left\{ \begin{array}{l} \sum_{s=1}^{2} Q_{ns} J_0(k_{rns} r) \cos(k_{zn} z) \\ \sum_{s=1}^{2} Q_{ns} \chi_{ns} J_1(k_{rns} r) \sin(k_{zn} z) \end{array} \right\}$$

in Eq. (5c) is replaced by

$$\left\{ \begin{array}{l} U_2 \\ W_2 \end{array} \right\} = \left\{ \begin{array}{l} Q_{n1} \cos(K_1 z) \\ 0 \end{array} \right\} + \left\{ \begin{array}{l} 0 \\ Q_{n2} J_1(K_1 r) \end{array} \right\} \tag{17a}$$

at $\omega = k_{zn} c_1$ and by

$$\left\{ \begin{array}{l} U_2 \\ W_2 \end{array} \right\} = \left\{ \begin{array}{l} Q_{n1} J_0(K_2 r) \\ 0 \end{array} \right\} + \left\{ \begin{array}{l} 0 \\ Q_{n2} \sin(K_2 z) \end{array} \right\} \tag{17b}$$

at $\omega = k_{zn} c_2$. U, in the term that is replaced, contains an r-dependent term that is necessary to make the set of functions complete in the radial direction. However, in the replacement Eqs. (16a) and (17a), U is not a function of r. Therefore, the expression for U is not in terms of a complete set of functions. Similarly, W in the term to be replaced is not a function of z. In contrast, in Eqs. (16b) and (17b), U and W are functions of r and z, respectively. However, for example, T_{zz} obtained from Eqs. (16b) and (17b) is zero, and the expression for T_{zz} is, therefore, not in terms of a complete set of functions. Moreover, numerical difficulties are likely to arise in the neighbourhoods of these frequencies. These can be handled by using approximate expressions for functions in the neighbourhoods. In a much simpler alternative method, computations are done using two different complete sets of functions. The frequencies at which difficulties occur are listed for each set and results obtained using the other set are used at these frequencies.

Another type of difficulty can occur on the boundary at other frequencies. For any chosen set of functions, there are frequencies at which $\cos(k_{zns} L/2)$ is zero. It is seen from equation (5b) that the corresponding axial displacement is zero on the flat surface. Similarly, at the frequencies at which $J_1(k_{rns} a)$ is zero, it is seen from Eq. (5c) that the corresponding radial displacement is zero on the curved surface. Therefore, the response to arbitrary excitations cannot be determined at such frequencies using the chosen set of functions. Again, the response is best computed using an alternative complete set of functions.

These difficulties will occur only for lossless cylinders with real Lame's constants. In cylinders with internal loss, Lame's constants are complex and these difficulties do not occur because there is no real frequency at which, for example, $\omega = k_{rn} c_1$ or $\cos(k_{zns} L/2) = 0$.

3. Special cases

Several special cases are presented to illustrate the procedure to analyse the free and forced vibrations of cylinders. The same set of functions that is complete in the radial direction is used in all cases. However, two different sets are used in the axial direction. The set of functions (set I) that is complete in the axial direction and obtained using Eq. (13) is used in cases 1A, 1B, 1C, 1D and 1E. In cases 2A and 2B, the set of functions (set II) defined in Eq. (14) is used. Zero displacement boundary conditions are used in cases 1A and 2A and the

same results are obtained even though different sets are used. Similarly, the same results are obtained in cases 1B and 2B where zero stress boundary conditions are used. In some cases, displacement is specified on the surface and, in other cases, stress is specified. Mixed boundary conditions where stress is specified over part of one surface and displacement is specified over the remaining part of the surface are not considered here.

Let the axial and radial displacements on the flat surfaces be denoted by $\bar{U}$ and $\bar{W}$, respectively, i.e.,

$$U = \bar{U} \quad \text{and} \quad W = \bar{W} \quad \text{on} \quad 0 \leqslant r \leqslant a, \quad z = \pm L/2. \tag{18a,b}$$

The boundary condition on $\bar{U}$ in Eq. (18a) is satisfied by using the orthogonal property of $J_0(k_{rn}a)$. Substituting Eq. (18a) in Eq. (5a), multiplying both sides by $r\,J_0(k_{rn}a)$ and integrating over r, yields

$$P\left[\frac{a^2}{2}\cos\left(\frac{K_1 L}{2}\right)\right] + Q\left[\frac{aJ_1(K_2 a)}{K_2}\right] + \sum_{m=1}^{M_z}\sum_{s=1}^{2} Q_{ms}\cos\left(\frac{k_{zm}L}{2}\right)\frac{aJ_1(k_{rms}a)}{k_{rms}} = \int_0^a \bar{U} r\,\mathrm{d}r, \quad n = 0 \tag{19a}$$

and

$$\sum_{s=1}^{2} P_{ns}\cos\left(\frac{k_{zns}L}{2}\right)R_0(k_{rn}) + QR_0(K_2) + \sum_{m=1}^{M_z}\sum_{s=1}^{2} Q_{ms}\cos\left(\frac{k_{zm}L}{2}\right)R_0(k_{rms}) = \int_0^a \bar{U}J_0(k_{rn}r)r\,\mathrm{d}r, \quad n = 1,2,\ldots \tag{19b}$$

by using [15]

$$\int_0^a rJ_0(Xr)J_0(k_{rn}r)\,\mathrm{d}r = R_0(X), \tag{20a}$$

where

$$R_0(X) = \begin{cases} 0, & X = k_{rm}, \quad m \neq n, \\ \dfrac{a^2}{2}J_0^2(k_{rn}a), & X = k_{rn}, \quad m = n, \\ \dfrac{Xa}{X^2 - k_{rn}^2}J_0(k_{rn}a)J_1(Xa), & X \neq k_{rn}, \quad n = 1,2,3,\ldots\,. \end{cases} \tag{20b}$$

The boundary condition on $\bar{W}$ in Eq. (18b) is satisfied by substituting it in Eq. (5a), and using the orthogonal property of $J_1(k_{rn}r)$. Multiplying both sides of Eq. (5a) by $rJ_1(k_{rn}r)$ and integrating over r yields

$$\sum_{s=1}^{2} P_{ns}\psi_{ns}\sin\left(\frac{k_{zns}L}{2}\right)R_1(k_{rn}) + \sum_{m=1}^{M_z}\sum_{s=1}^{2} Q_{ms}\chi_{ms}\sin\left(k_{zm}L/2\right)R_1(k_{rms}) = \int_0^a \bar{W}J_1(k_{rn}r)r\,\mathrm{d}r, \quad n = 1,2,\ldots. \tag{21}$$

Eq. (21) is obtained by using [15]

$$\int_0^a rJ_1(Xr)J_1(k_{rn}r)\,\mathrm{d}r = R_1(X), \tag{22a}$$

where

$$R_1(X) = \begin{cases} 0, & X = k_{rm}, \quad m \neq n, \\ \dfrac{a^2}{2}J_0^2(k_{rn}a), & X = k_{rn}, \quad m = n, \\ \dfrac{k_{rn}a}{X^2 - k_{rn}^2}J_0(k_{rn}a)J_1(Xa), & X \neq k_{rn}, \quad n = 1,2,3,\ldots\,. \end{cases} \tag{22b}$$

Let the axial and radial displacements on the curved surface be denoted by $\hat{U}$ and $\hat{W}$, respectively, i.e.,

$$U = \hat{U} \quad \text{and} \quad W = \hat{W} \quad \text{on} \quad r = a, |z| \leqslant L/2. \tag{23a,b}$$

The boundary condition on $\hat{U}$ in Eq. (23a) is satisfied by substituting it in Eq. (5a) and using the orthogonal property of $\cos(k_{zm}z)$ in Eq. (15b). Multiplying both sides of Eq. (5a) by $\cos(k_{zn}z)$ and integrating over z yields

$$P\left[\frac{2}{K_1}\sin\left(\frac{K_1 L}{2}\right)\right] + Q[J_0(K_2 a)L] + \sum_{m=1}^{M_r}\sum_{s=1}^{2} P_{ms}\left[\frac{2J_0(k_{rm}a)}{k_{zms}}\sin\left(\frac{k_{zms}L}{2}\right)\right] = \int_{-L/2}^{L/2} \hat{U}\,\mathrm{d}z, \quad n = 0 \tag{24a}$$

and

$$PS_c(K_1) + \sum_{m=1}^{M_r}\sum_{s=1}^{2} P_{ms}J_0(k_{rm}a)S_c(k_{zms}) + \sum_{s=1}^{2} Q_{ns}J_0(k_{rns}a)S_c(k_{zn}) = \int_{-L/2}^{L/2} \hat{U}\,\cos(k_{zn}z)\,\mathrm{d}z, \quad n = 1, 2, \ldots \tag{24b}$$

by using

$$\int_{-L/2}^{+L/2} \cos(Xz)\cos(k_{zn}z)\,\mathrm{d}z = S_c(X), \tag{25a}$$

where

$$S_c(X) = \begin{cases} 0, & X = k_{zm}, \quad m \neq n, \\ L/2, & X = k_{zn}, \quad m = n, \\ 2\left[\dfrac{k_{zn}\sin\left(k_{zn}L/2\right)\cos\left(XL/2\right) - X\cos\left(k_{zn}L/2\right)\sin\left(XL/2\right)}{\left(k_{zn}^2 - X^2\right)}\right], & X \neq k_{zn}, \quad n = 1, 2, 3, \ldots. \end{cases} \tag{25b}$$

The boundary condition on $\hat{W}$ in Eq. (23b) is satisfied by substituting it in Eq. (5a) and using the orthogonal property of $\sin(k_{zm}z)$ in Eq. (15a). Multiplying both sides of Eq. (5a) by $\sin(k_{zn}z)$and integrating over z yields

$$\frac{L}{2}\sum_{s=1}^{2} Q_{ns}\chi_{ns}J_1(k_{rns}a) = \int_{-L/2}^{L/2} \hat{W}\,\sin(k_{zn}z)\,\mathrm{d}z, \quad n = 1, 2, \ldots. \tag{26}$$

Next, consider the case where stresses are specified on the boundary. Let the normal and shear stress on the flat surfaces be denoted by $\bar{T}_{zz}$ and $\bar{T}_{rz}$, respectively, and the normal and shear stress on the curved surface be denoted by $\widehat{T_{rr}}$ and $\widehat{T_{rz}}$, respectively, i.e.,

$$T_{zz} = \bar{T}_{zz} \quad \text{and} \quad T_{rz} = \bar{T}_{rz} \quad \text{on} \quad 0 \leqslant r \leqslant a, z = \pm L/2 \tag{27a,b}$$

and

$$T_{rr} = \widehat{T_{rr}} \quad \text{and} \quad T_{rz} = \widehat{T_{rz}} \quad \text{on} \quad r = a, |z| \leqslant L/2. \tag{27c,d}$$

The boundary condition on T_{zz} in Eq. (27a) is satisfied by using the orthogonal property of $J_0(k_{rn}a)$ in Eq. (12). Substituting Eq. (27a) in Eq. (10), multiplying both sides by $rJ_0(k_{rn}a)$ and integrating over r, yields

$$\begin{aligned} &-P\left[(\lambda + 2\mu)\frac{K_1 a^2}{2}\sin\left(\frac{K_1 L}{2}\right)\right] \\ &+\sum_{m=1}^{M_z}\sum_{s=1}^{2} Q_{ms}\sin\left(k_{zm}L/2\right)\left[-(\lambda + 2\mu)k_{zm} + \lambda\chi_{ms}k_{rms}\right]\frac{a}{k_{rms}}J_1(k_{rms}a) = \int_0^a \bar{T}_{zz}r\,\mathrm{d}r, \quad n = 0 \end{aligned} \tag{28a}$$

and

$$\sum_{s=1}^{2} P_{ns}\sin\left(\frac{k_{zns}L}{2}\right)\left[-(\lambda+2\mu)k_{zns}+\lambda\psi_{ns}k_{rn}\right]R_0(k_{rn}) + \sum_{m=1}^{M_z}\sum_{s=1}^{2} Q_{ms}\sin\left(k_{zm}L/2\right)\left[-(\lambda+2\mu)k_{zm}+\lambda\chi_{ms}k_{rms}\right]R_0(k_{rms}) = \int_0^a \bar{T}_{zz}J_0(k_{rn}r)r\,\mathrm{d}r, \quad n=1,2,\ldots. \tag{28b}$$

by using Eq. (18).

The boundary condition on T_{rz} in Eq. (27b) is satisfied by substituting it in Eq. (11), and using the orthogonal property of $J_1(k_{rn}r)$in Eq. (12). Multiplying both sides of Eq. (11) by $rJ_1(k_{rn}r)$ and integrating over r yields

$$\mu\frac{a^2}{2}J_0^2(k_{rn}a)\sum_{s=1}^{2} P_{ns}\left[\psi_{ns}k_{zns}-k_{rn}\right]\cos\left(k_{zns}L/2\right) + \mu\sum_{m=1}^{M_z}\sum_{s=1}^{2} Q_{ms}\left[+\chi_{ms}k_{zm}-k_{rms}\right]R_1(k_{rms}) = \int_0^a \bar{T}_{rz}rJ_1(k_{rn}r)\,\mathrm{d}r, \quad n=1,2,\ldots. \tag{29}$$

The boundary condition on T_{rr} in Eq. (27c) is satisfied by substituting it in Eq. (9) and using the orthogonal property of $\sin(k_{zm}z)$. Multiplying both sides of Eq. (9) by $\sin(k_{zn}z)$and integrating over z yields

$$-PK_1\lambda S_s(K_1)+\sum_{m=1}^{M_r}\sum_{s=1}^{2} P_{ms}\left[(\lambda+2\mu)\psi_{ms}k_{rm}-\lambda k_{zms}\right]J_0(k_{rm}a)S_s(k_{zms}) + \sum_{s=1}^{2} Q_{ns}\left\{\left[(\lambda+2\mu)\chi_{ns}k_{rns}-\lambda k_{zn}\right]J_0(k_{rns}a)-\frac{2\mu}{a}\chi_{ns}J_1(k_{rns}a)\right\}L/2 = \int_{-L/2}^{L/2}\widehat{T_{rr}}\,\sin(k_{zn}z)\,\mathrm{d}z, \quad n=1,2,\ldots \tag{30}$$

by using

$$\int_{-L/2}^{+L/2}\sin(Xz)\sin(k_{zn}z)\,\mathrm{d}z = S_s(X), \tag{31a}$$

where

$$S_s(X)=\begin{cases} 0 & X=k_{zm}, \quad m\neq n, \\ L/2 & X=k_{zn}, \quad m=n, \\ 2\left[\dfrac{X\sin\left(k_{zn}L/2\right)\cos\left(XL/2\right)-k_{zn}\cos\left(k_{zn}L/2\right)\sin\left(XL/2\right)}{\left(k_{zn}^2-X^2\right)}\right] & X\neq k_{zn}, \quad n=1,2,3,\ldots. \end{cases} \tag{31b}$$

The boundary condition on T_{rz} in Eq. (27d) is satisfied by substituting it in Eq. (11) and using the orthogonal property of $\cos(k_{zm}z)$ in Eq. (15b). Multiplying both sides of Eq. (11) by $\cos(k_{zn}z)$ and integrating over z yields

$$\mu L/2\sum_{s=1}^{2} Q_{ns}\left[\chi_{ns}k_{zn}-k_{rns}\right]J_1(k_{rns}a) = \int_{-L/2}^{L/2}\widehat{T_{rz}}\,\cos(k_{zn}z)\,\mathrm{d}z, \quad n=1,2,\ldots. \tag{32}$$

For each particular case, the relevant equations are combined, truncated, and expressed in matrix form. When set I is used, Q is set to zero and the final equation has the form

$$[\mathbf{F}]\{\mathbf{X}\}=\{\mathbf{G}\}, \tag{33a}$$

where

$$\{\mathbf{X}\}^{\mathrm{T}}=\left[P,P_{11},P_{12},P_{21},P_{22},\ldots,P_{M_r1},P_{M_r2},Q_{11},Q_{12},Q_{21},Q_{22},\ldots,Q_{M_z1},Q_{M_z2}\right]. \tag{33b}$$

[**F**] is a square matrix of size $[2(M_r+M_z)+1,\ 2(M_r+M_z)+1]$, and M_r and M_z are now finite. The elements of the column matrix $\{\mathbf{G}\}$ are zero when the specified displacement or stress is zero on the boundary. When set II is used, Q is non-zero and the final equation has the form shown in Eq. (33) but

$$\{\mathbf{X}\}^{\mathrm{T}} = \left[P, Q, P_{11}, P_{12}, P_{21}, P_{22}, \ldots, P_{M_r1}, P_{M_r2}, Q_{11}, Q_{12}, Q_{21}, Q_{22}, \ldots, Q_{M_z1}, Q_{M_z2}\right] \tag{33c}$$

and [**F**] is a square matrix of size $[2(M_r+M_z)+2,\ 2(M_r+M_z)+2]$.

3.1. Case 1A

Set I is used here. The displacements on the boundaries are zero, i.e.,

$$\bar{U}=0 \quad \text{and} \quad \bar{W}=0 \quad \text{on} \quad 0\leqslant r\leqslant a, z=\pm L/2 \tag{34a,b}$$

and

$$\widehat{U}=0 \quad \text{and} \quad \widehat{W}=0 \quad \text{on} \quad r=a, |z|\leqslant L/2. \tag{34c,d}$$

Eqs. (19)–(26) are assembled to form [**F**] after setting $Q=0$. All the elements of $\{\mathbf{G}\}$ are zero. For lossless cylinders, the resonance frequencies are determined by finding the frequencies at which solutions to the homogeneous matrix equation exist.

3.2. Case 1B

Set I is used here. The stresses on all the surfaces are zero, i.e.,

$$\bar{T}_{zz}=0 \quad \text{and} \quad \bar{T}_{rz}=0 \quad \text{on} \quad 0\leqslant r\leqslant a, z=\pm L/2 \tag{35a,b}$$

and

$$\widehat{T}_{rr}=0 \quad \text{and} \quad \widehat{T}_{rz}=0 \quad \text{on} \quad r=a, |z|\leqslant L/2. \tag{35c,d}$$

Eqs. (28)–(32) are assembled to form [**F**]. All the elements of $\{\mathbf{G}\}$ are zero. For lossless cylinders, the resonance frequencies are determined by finding the frequencies at which solutions to the homogeneous matrix equation exist.

3.3. Case 1C

Set I is used to determine the response to forced vibration. The stress on the surfaces, except $\bar{T}_{zz}$ inside a circle of radius a/N, is zero everywhere, i.e.,

$$\bar{T}_{zz}=\left\{\begin{array}{ll} \pm 1 & \text{on} \quad 0\leqslant r\leqslant a/N, \quad z=\pm L/2 \\ 0 & \text{on} \quad a/N<r\leqslant a, \quad z=\pm L/2 \end{array}\right\}, \tag{36a}$$

$$\bar{T}_{rz}=0, \quad \widehat{T}_{rz}=0 \tag{36b, 36c}$$

and

$$\widehat{T}_{rr}=0. \tag{36d}$$

Eqs. (28)–(32) are assembled to form [**F**]. It therefore follows that the non-zero elements of $\{\mathbf{G}\}$ are

$$G_1=\int_0^a \bar{T}_{zz} r\,\mathrm{d}r=\frac{a^2}{2N^2}, \tag{37a}$$

$$G_{n+1}=\int_0^a \bar{T}_{zz} J_0(k_{rn}r) r\,\mathrm{d}r=\frac{a}{Nk_{rn}}\left[J_1\left(\frac{k_{rn}a}{N}\right)\right], \quad n=1,2,\ldots,M_r. \tag{37b}$$

3.4. Case 1D

Set I is used here. The stress on the surfaces, except $\bar{T}_{zz}$ outside a circle of radius a/N, is zero everywhere i.e., the boundary conditions are

$$\overline{T}_{zz} = \left\{ \begin{matrix} 0 & \text{on} & 0 \leqslant r \leqslant a/N, & z = \pm L/2 \\ \pm 1 & \text{on} & a/N < r \leqslant a, & z = \pm L/2 \end{matrix} \right\} \tag{38}$$

and Eqs. (36b)–(36d).

Eqs. (28)–(32) are assembled to form [**F**]. It therefore follows that the non-zero elements of {**G**} are

$$G_1 = \int_0^a \bar{T}_{zz} r \, \mathrm{d}r = \frac{a^2(N^2-1)}{2N^2}, \tag{39a}$$

$$G_{n+1} = \int_0^a \bar{T}_{zz} J_0(k_{rn} r) r \, \mathrm{d}r = -\frac{a}{N k_{rn}} J_1\left(\frac{k_{rn} a}{N}\right), \quad n = 1, 2, \ldots, M_r. \tag{39b}$$

3.5. Case 1E

Set I is used. The stresses on the surfaces, except $\widehat{T}_{rr}$ inside a band, are zero everywhere i.e., the boundary conditions are

$$\bar{T}_{zz} = 0 \ \text{ on } \ 0 \leqslant r \leqslant a, \quad z = \pm L/2. \tag{40a}$$

Eqs. (34b) and (34c), and

$$\widehat{T}_{rr} = \left\{ \begin{matrix} \Gamma z & \text{on} & r = a, & |z| \leqslant L/2N, \\ 0 & \text{on} & r = a, & L/2N < |z| \leqslant L/2, \end{matrix} \right. \tag{40b}$$

where Γ is a constant.

The only non-zero elements of {**G**} are

$$G_{2M_r+n+1} = \int_{-L/N}^{L/N} \widehat{T}_{rr} \cos(k_{zn} z) \, \mathrm{d}z = \frac{2}{k_{zn}^2} \sin\left(\frac{k_{zn} L}{2N}\right) - \frac{L}{N k_{zn}} \cos\left(\frac{k_{zn} L}{2N}\right), \quad n = 1, 2, \ldots, M_z. \tag{41}$$

3.6. Case 2A

In this case, set II is used. All the displacements are zero on the boundary. The same boundary conditions are considered in case 1A where set I is used. Here, Eq. (33c) is used whereas Eq. (33b) is used in case 1A. All the elements of {**G**} are zero.

3.7. Case 2B

In this case, set II is used. All the stresses are zero on the boundary. The same boundary conditions are considered in Case 1B where set I is used. Both P and Q are zero here because of the boundary conditions.

4. Numerical results and discussion

Numerical results are presented for a solid elastic cylinder with density 7800 kg/m^3. Free vibration results are presented for a cylinder with Young's modulus, $Y = 200$ GPa and Poisson's ratio, $\sigma = 0.3$, i.e., the Lame's constants are $\lambda \approx 115.38$ GPa and $\mu \approx 76.923$ GPa, respectively. Forced vibration results are presented for a

cylinder with length and diameter 10 mm each and internal losses: $Y = 200(1 + j0.01)$ GPa and $\sigma = 0.3$. These complex material properties satisfy the conditions derived in the appendix. Solid lines and dots are used to show forced responses obtained using the present approach and ATILA, respectively. In the present approach $M_r = M_z = 20$ is used to obtain the forced responses shown in most of the figures. In ATILA, 8 noded,

Table 1
Resonance frequencies of a cylinder of length and diameter 10 mm each computed using various methods for case 1A. All displacements are zero on the boundaries.

Mode no.	Resonance frequency (kHz)				
	ATILA [12] $I = J = 40$	Present method			
		$M_r = M_z = 1$	$M_r = M_z = 5$	$M_r = M_z = 10$	$M_r = 10$, $M_z = 20$
1	361.408	361.020	361.399	361.406	361.407
2	579.222	575.371	579.219	579.221	579.221
3	682.230		682.226	682.229	682.229
4	819.557		819.526	819.552	819.554
5	876.031		875.975	876.022	876.026

Table 2
Resonance frequencies of a cylinder of length 20 mm and diameter 10 mm computed using various methods for case 1A. All displacements are zero on the boundaries.

Mode no.	Resonance frequency (kHz)					
	Hutchinson [16]	ATILA [12] $I = J = 40$	Present method			
			$M_r = M_z = 1$	$M_r = M_z = 5$	$M_r = M_z = 10$	$M_r = 10$, $M_z = 20$
1	275.447	275.448	275.377	275.441	275.447	275.448
2	453.402	453.404		453.364	453.399	453.403
3	556.637	556.637	554.398	556.636	556.637	556.637
4	595.994	595.996		595.955	595.992	595.995

Table 3
Resonance frequencies of a lossless cylinder of length and diameter 10 mm each computed using various methods for case 1B. All stresses are zero on the boundaries.

Mode no.	Resonance frequency (kHz)					
	Gladwell and Vijay [17]	Leissa and So [18]	ATILA [12] $I = J = 40$	Present method		
				$M_r = M_z = 5$	$M_r = M_z = 10$	$M_r = M_z = 15$
1	287.11	287.09	287.06	287.38	287.15	287.11
2	354.12	353.96	353.99	354.84	354.22	354.10
3	471.28	470.52	470.53	470.98	470.66	470.59
4	548.99	547.89	547.89	548.06	547.94	547.92
5		622.36	622.32	625.38	623.14	622.70
6			661.93	662.14	661.99	661.96
7			720.31	721.42	720.62	720.46
8			810.50	810.98	810.64	810.57
9			821.22	821.52	821.30	821.26
10			909.10	915.94	910.90	909.93
11			985.94	987.28	986.31	986.11

axisymmetric, rectangular, quadratic elements are used to model the cylinder. I elements are used along the length of the cylinder and J elements are used in the radial direction. Only half the cylinder is modelled and the radial displacement and T_{zz} are prescribed to be zero on $z = 0$ to simulate the full cylinder. Forced responses are computed at frequencies that are less than or equal to 1 MHz and integer multiples of 10 kHz.

The resonance frequencies that are less than 1 MHz of a lossless cylinder of length and diameter 10 mm each with zero displacement on the surfaces are shown in Table 1. The convergence of the resonance frequencies, for case 1A, is illustrated by presenting results for various values of M_r and M_z. They are obtained by finding the zeros in the determinant of [**F**] and compared with the results obtained using ATILA. The difference between frequencies obtained using the present method and ATILA is less than 0.01% even when $M_r = M_z = 5$ and is in the sixth significant digit when $M_r = M_z = 20$. There are discontinuities in the determinant at approximately 294, 414, 607, 845, 874, and 881 kHz. These frequencies correspond to k_{r11}, $\cos(k_{z12}L/2)$, $\cos(k_{z12}L/2)$, $\cos(k_{z22}L/2)$, $\cos(k_{z12}L/2)$, and $k_{r21} = 0$, respectively. (As noted earlier, k_{zmn} and k_{rmn} are frequency dependent.)

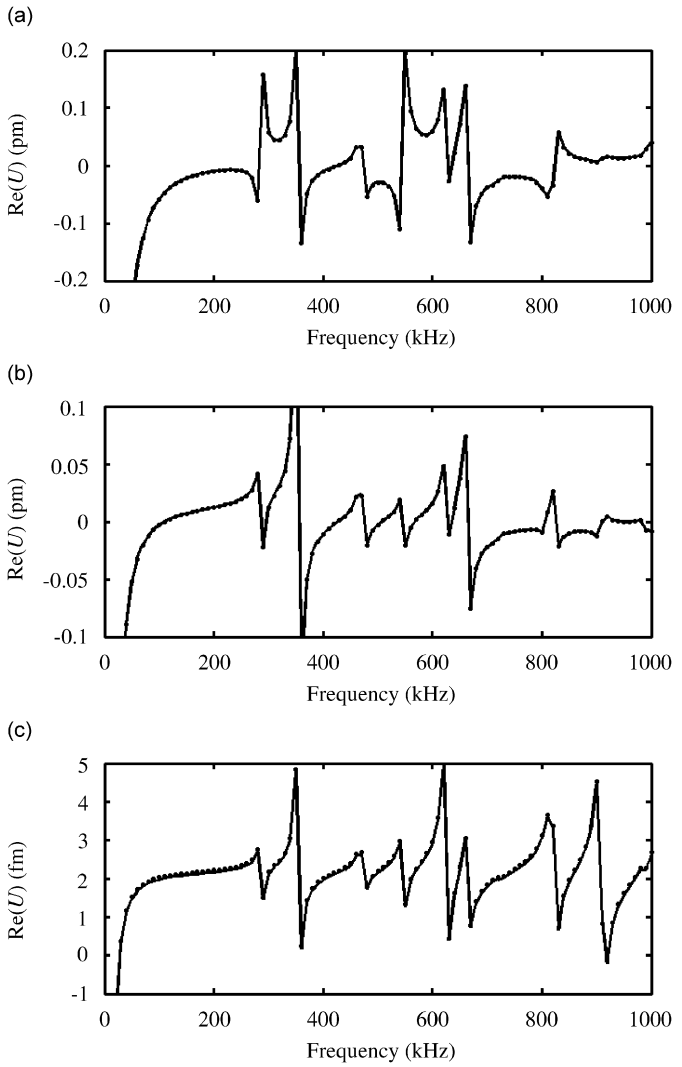

Fig. 2. Axial displacement, Re(U), at $r = 0$, $z = L/2$ for case 1C. Solid line: present method, dots: ATILA. (a) $N = 1$, $M_r = M_z = 20$; 1600 elements (b) $N = 2$, $M_r = M_z = 20$; 1600 elements, and (c) $N = 20$, $M_r = M_z = 50$; 2500 elements.

Hutchinson [16] tabulated normalised results for a cylinder with a length to diameter ratio of two. Therefore, resonance frequencies of a cylinder of length 20 mm and diameter 10 mm are presented in Table 2 for case 1A. Even the sixth significant digit is in agreement or differs by one from the results of Hutchinson and ATILA.

The resonance frequencies for case 1B that are less than 1 MHz, obtained by using various values of M_r and M_z, are shown in Table 3. Resonance frequencies obtained by Gladwell and Vijay [17], Leissa and So [18] and ATILA [12] are also shown in Table 3. Gladwell and Vijay used only a few elements. In ATILA, 1600 square elements are used. In most cases, the difference in the resonance frequencies obtained using the present method and ATILA is much less than 0.8%, even when $M_r = M_z = 5$.

The axial displacement, U, at $r = 0$, $z = L/2$ is shown in Figs. 2(a)–(c) for case 1C, $N = 1$, 2, and 20, respectively. The agreement is good. For $N = 1$ and 2, ATILA results are obtained by using 1600 square, equisized elements and $M_r = M_z = 20$ is used in the present method. For $N = 20$, 2500 elements are used in ATILA and $M_r = M_z = 50$ is used in the present method.

The effect of M_r and M_z on the computed axial displacement, U, at $r = 0$, $z = L/2$, is shown in Table 4 for Case 1C, $N = 1$, 2, and 20 at 100, 200,…,1000 kHz. For $N = 1$, and $M_r = M_z = 10$ there is a difference, in most cases, only in the third significant digit of the displacements computed using the present method and ATILA. For $N = 2$, $M_r = M_z = 20$ yields results with similar accuracy. When N increases, the load is more concentrated and the number of terms required for obtaining a similar relative accuracy also increases.

Table 4
Axial displacement, Re(U), at $r = 0$, $z = L/2$ for case 1C

N	Frequency (kHz)	Axial displacement, Re(U) (fm)				
		ATILA [12]	Present method			
			$M_r = M_z = 5$	$M_r = M_z = 10$	$M_r = M_z = 20$	$M_r = M_z = 50$
1	100	−58.45	−58.53	−58.41	−58.44	−58.45
	200	−10.36	−10.45	−10.30	−10.34	−10.35
	300	56.48	58.16	56.14	56.33	56.44
	400	−10.91	−12.18	−10.91	−10.89	−10.90
	500	−29.10	−28.49	−29.22	−29.15	−29.11
	600	59.27	55.50	58.80	59.20	59.28
	700	−38.68	−38.70	−38.26	−38.55	−38.65
	800	−40.12	−40.52	−39.98	−40.08	−40.11
	900	5.08	7.01	5.83	5.29	5.12
	1000	38.83	37.48	38.87	38.85	38.84
2	100	−3.035	−2.74	−2.80	−3.15	−3.01
	200	12.53	12.86	12.74	12.41	12.55
	300	12.82	13.05	13.09	12.72	12.85
	400	−10.58	−11.87	−10.32	−10.66	−10.54
	500	−2.58	−2.41	−2.29	−2.67	−2.55
	600	15.66	14.69	15.79	15.54	15.69
	700	−21.98	−21.64	−21.41	−22.00	−21.94
	800	−9.13	−9.23	−8.26	−9.05	−9.06
	900	−12.83	−10.6	−11.99	−12.80	−12.78
	1000	−8.07	−6.22	−7.75	−8.17	−8.05
20	100	2.03	0.74	1.46	2.19	1.97
	200	2.22	0.94	1.65	2.39	2.16
	300	2.18	0.88	1.61	2.34	2.12
	400	2.00	0.67	1.44	2.17	1.95
	500	2.20	0.89	1.63	2.37	2.15
	600	2.96	1.54	2.33	3.12	2.90
	700	1.84	0.49	1.25	2.00	1.78
	800	3.12	1.77	2.53	3.28	3.06
	900	4.53	2.39	3.62	4.61	4.46
	1000	2.69	1.20	2.10	2.86	2.63

It is seen from Eqs. (33) and (37) as well as from Table 4 that the values of M_r and M_z required to get reasonable accuracy depends primarily on the spatial distribution of the excitation and to a lesser extent on the frequency of excitation.

The real and imaginary parts of the axial displacement are shown in Fig. 3 in the neighbourhood of the first resonance frequency for case 1C. The maxima and the minima and the frequencies at which they occur are in good agreement with ATILA. This indicates that methods [19] used to determine real material properties can be extended to determine the complex material properties of cylinders with internal loss.

The axial displacement, Re(U), at $r = 0$, $z = L/2$ is shown in Fig. 4 and Table 5 for case 1D, $N = 2$. As expected, the sum of the responses to the excitations in cases 1C and 1D, $N = 2$ is equal to the response to the excitation in case 1C, $N = 1$, i.e., the sum of the responses to excitations inside and outside a circle of radius $a/2$ is equal to the response to the excitation over a circle of radius a.

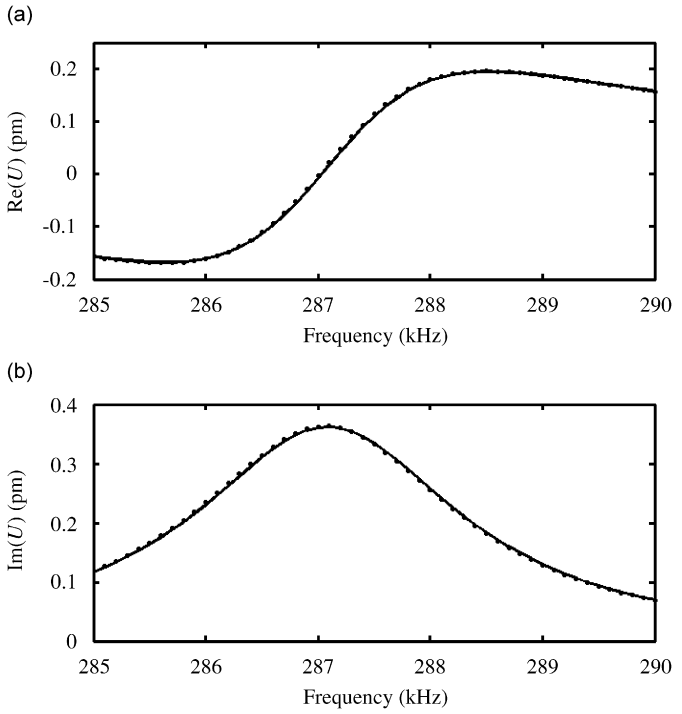

Fig. 3. Axial displacement, U, at $r = 0$, $z = L/2$ for case 1C, $N = 1$, in the neighbourhood of the first resonance. Solid line: present method, dots: ATILA.

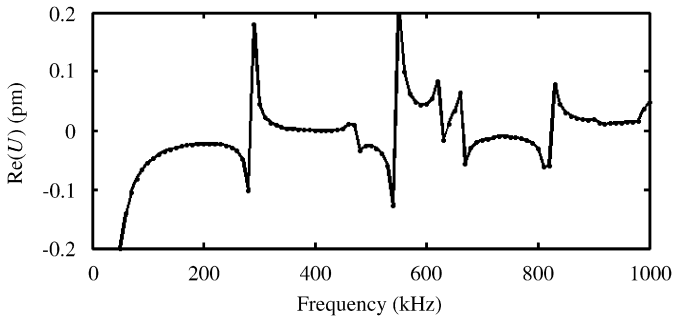

Fig. 4. Axial displacement, Re(U), at $r = 0$, $z = L/2$ for case 1D, $N = 2$. Solid line: present method using $M_r = M_z = 20$, dots: ATILA.

Table 5
Axial displacement, Re(U), at $r = 0$, $z = L/2$ for case 1D

N	Frequency (kHz)	Axial displacement, U (fm)				
		ATILA [12]	Present method			
			$M_r = M_z = 5$	$M_r = M_z = 10$	$M_r = M_z = 20$	$M_r = M_z = 50$
2	100	−55.42	−55.79	−55.61	−55.29	−55.44
	200	−22.89	−23.30	−23.04	−22.74	−22.91
	300	43.66	45.11	43.05	43.61	43.59
	400	−0.326	−0.308	−0.589	−0.229	−0.354
	500	−26.52	−26.08	−26.92	−26.47	−26.56
	600	43.61	40.81	43.01	43.65	43.59
	700	−16.69	−17.06	−16.85	−16.55	−16.71
	800	−30.99	−31.29	−31.72	−31.04	−31.05
	900	17.90	17.60	17.82	18.09	17.89
	1000	46.90	43.70	46.62	47.02	46.89

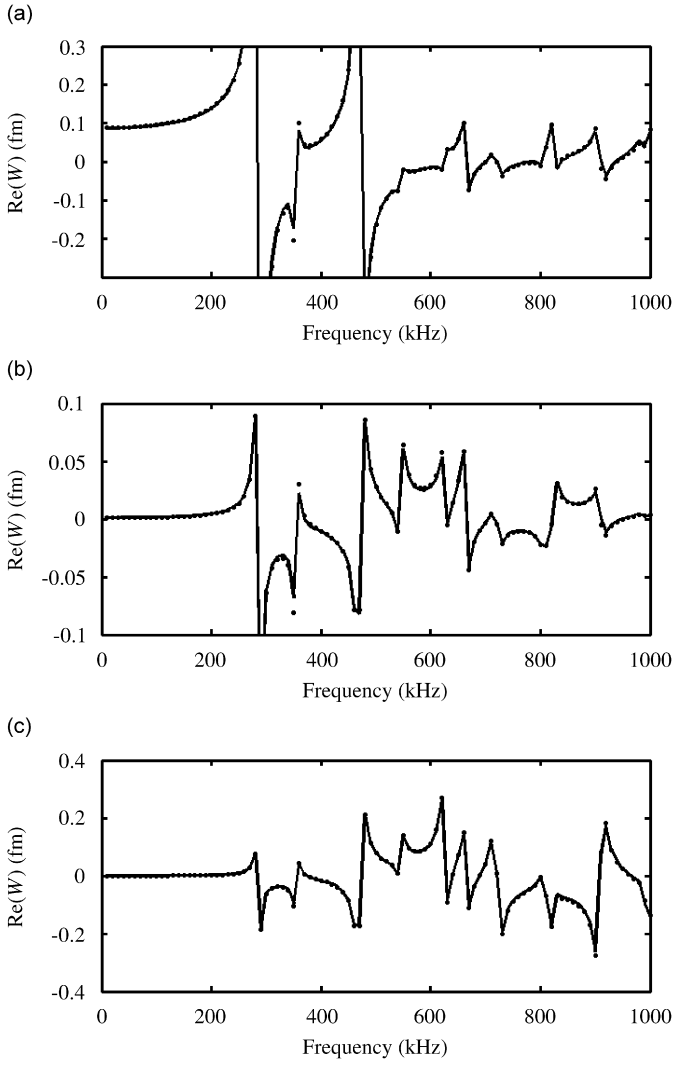

Fig. 5. Radial displacement, W, at $r = a$, $z = L/2$ for case 1E. Solid line: present method, dots: ATILA (a) $N = 1$, $\Gamma = 1$, $M_r = M_z = 20$ (b) $N = 2$, $\Gamma = 1$, $M_r = M_z = 20$ (c) $N = 20$, $\Gamma = 103$, $M_r = M_z = 50$.

The radial displacement, Re(W), at $r = a$, $z = L/2$ is shown in Fig. 5 and Table 6 for case 1E, $N = 1$, 2, and 20. The values of Γ are not the same and are chosen for convenient presentation. In this case also, higher values of M_r and M_z are needed to get good agreement with ATILA when the load is concentrated.

Table 6
Radial displacement, Re(W), at $r = a$, $z = L/2$ for case 1E

Excitation N	Frequency (kHz)	Radial displacement, Re(W) (fm)				
		ATILA [12]	Present method			
			$M_r = M_z = 20$	$M_r = M_z = 50$	$M_r = M_z = 100$	$M_r = M_z = 200$
$N = 1$, $\Gamma = 1$	100	95.40	94.20	94.92	95.16	95.28
	200	139.5	137.8	138.8	139.2	139.4
	300	−516.9	−506.0	−512.3	−514.6	−515.7
	400	58.59	54.45	56.93	57.76	58.17
	500	−163.0	−160.5	−162.0	−162.5	−162.8
	600	−14.72	14.73	−14.73	−14.73	−14.72
	700	−1.368	−1.50	−1.42	−1.393	−1.380
	800	−11.58	−7.77	−10.1	−10.82	−11.20
	900	86.94	76.9	83.4	85.24	86.12
	1000	83.25	74.8	79.9	81.56	82.41
$N = 2$, $\Gamma = 10^3$	100	1.341	1.56	1.403	1.378	1.359
	200	4.111	4.39	4.195	4.159	4.135
	300	−63.88	−61.95	−63.09	−63.47	−63.67
	400	−10.58	−11.51	−10.98	−10.77	−10.68
	500	27.68	26.71	27.26	27.48	27.58
	600	29.35	27.18	28.48	28.93	29.14
	700	−3.941	−3.843	−3.930	−3.929	−3.938
	800	−22.14	−22.07	−22.15	−22.14	−22.14
	900	−25.92	23.51	25.02	25.50	25.72
	1000	−4.019	3.329	3.715	3.874	3.947
$N = 20$, $\Gamma = 10^6$	100*	8.76	4.69	8.85	8.59	8.75
	200	1.60	−1.72	1.63	1.51	1.66
	300	−61.6	−62.7	−60.8	−61.3	−61.3
	400	−17.0	−22.0	−17.6	−17.4	−17.1
	500	79.2	73.2	78.0	78.5	79.0
	600	111.4	98.9	108.0	109.6	110.6
	700	41.5	36.4	40.9	41.1	41.4
	800	−4.59	−9.15	−5.01	−4.90	−4.64
	900	−275	−243	−262	−269	−272
	1000	−138	−156	−143	−141	−139

*$r = a$, $z = L/4$.

Table 7
Resonance frequencies of a cylinder of length and diameter 10 mm each for case 2A. All displacements are zero on all the boundaries.

Mode no.	Resonance frequency (kHz)				
	ATILA [12] $I = J = 40$	Present method			
		$M_r = M_z = 1$	$M_r = M_z = 5$	$M_r = M_z = 10$	$M_r = 10$, $M_z = 20$
1	361.408	360.622	361.384	361.404	361.405
2	579.222	575.550	579.215	579.220	579.221
3	682.230	673.890	682.215	682.228	682.229
4	819.557		819.469	819.542	819.548
5	876.031		875.915	876.009	876.017

Table 8
Resonance frequencies of cylinders of diameter 10 mm for case 2B. All stresses are zero on all the boundaries.

Length (mm)	Mode no.	Resonance frequency (kHz)		
		Thin rod theory	ATILA [12] $I = J = 40$	Present method $M_r = M_z = 5$
100	1	50.637	50.523	50.523
	2	101.274	100.315	100.315
	3	151.911	148.404	148.403
50	1	101.274	100.315	100.315
	2	202.548	193.250	193.251
	3	303.822	264.214	264.214
25	1	202.548	193.248	193.250
20	1	253.185	232.549	232.555

The resonance frequencies for case 2A that are less than 1 MHz, obtained by using various values of M_r and M_z, are compared in Table 7 with those obtained by using ATILA [12]. It is seen that there is good agreement. There is also excellent agreement between the resonance frequencies in Tables 1 and 7. The results are for the same boundary conditions but are obtained using two different complete sets of functions in the axial direction, i.e., sets I and II, respectively. In addition to the zeros listed in Table 7, there are discontinuities in the determinant at approximately 383, 495, 587, 701, and 768 kHz. These frequencies correspond to k_{z12}, $J_1(k_{r12}a)$, k_{r11}, k_{z22}, and $J_1(k_{r12}a)$, respectively $= 0$. It is seen that the frequencies at which discontinuities occur when set II is used are different from the frequencies when set I is used. This is important because some resonance frequencies of cylinders with certain length to radius ratio will be equal to the frequencies at which discontinuities occur. Therefore, this approach can be used to determine the resonance frequencies of lossless cylinders with all length to radius ratios. As noted earlier, these difficulties do not occur for cylinders with loss.

Resonance frequencies computed using thin rod theory, ATILA, and the present methods are compared in Table 8 for case 2B. The diameter of the cylinder is 10 mm in all the cases but the length is varied. Even when the length to diameter ratio is large, thin rod theory yields accurate results only for the lower order resonance frequencies. It is less accurate for the higher order modes of long thin rods and for shorter rods. However, there is good agreement between ATILA and the present method for all length to diameter ratios even when $M_r = M_z = 5$.

5. Conclusions

A method is presented to determine the response of solid cylinders with internal losses to distributed excitations. The method is based on the use of two infinite series solutions to the governing equations. Each term in the two series is an exact solution to the governing equations. The two series consist of terms that are orthogonal and form complete sets of functions in the axial and radial directions, respectively.

Numerical solutions are presented to illustrate free and forced vibration responses. Two different sets that are complete in the axial direction are used to compute the resonance frequencies of lossless cylinders. The results are in excellent agreement with each other and the results obtained using ATILA. It is seen that only a few terms of the infinite series are needed to compute several resonance frequencies as well as determine the response to high-frequency loads on the flat and curved surfaces of cylinders with internal losses. Results are presented for uniform and concentrated loads on the flat and curved surfaces.

The method can be extended to determine the responses of solid cylinders to excitations that are neither symmetric nor anti-symmetric about the plane midway between the ends of the cylinder. This can be done by expressing the displacements as the sum of the series used here and the sum of the series used in Ref. [2].

Appendix

The conditions that are satisfied by the imaginary parts of the complex Young's modulus, Y, and Poisson's ratio σ, are derived here by using the conditions derived by Holland [11] for piezoelectric material.

The relationship between stress and strain is given by the matrix Eq. (3) where

$$\lambda = \sigma Y/[(1+\sigma)(1-2\sigma)] \tag{A.1}$$

and

$$\mu = Y/[2(1+\sigma)]. \tag{A.2}$$

Eq. (3) can also be expressed as

$$[S_{rr}, S_{\theta\theta}, S_{zz}, S_{rz}]^{\mathrm{T}} = [S][T_{rr}, T_{\theta\theta}, T_{zz}, T_{rz}]^{\mathrm{T}}, \tag{A.3a}$$

where the square matrix $[S]$ is

$$[S] = \begin{bmatrix} \frac{1}{Y} & -\frac{\sigma}{Y} & -\frac{\sigma}{Y} & 0 \\ -\frac{\sigma}{Y} & \frac{1}{Y} & -\frac{\sigma}{Y} & 0 \\ -\frac{\sigma}{Y} & -\frac{\sigma}{Y} & \frac{1}{Y} & 0 \\ 0 & 0 & 0 & 2\frac{(1+\sigma)}{Y} \end{bmatrix}. \tag{A.3b}$$

The Young's modulus and the Poisson's ratio can be expressed in complex form as

$$Y = Y' + jY'' \tag{A.4}$$

and

$$\sigma = \sigma' + j\sigma'', \tag{A.5}$$

respectively. The imaginary terms should dissipative energy, hence the imaginary elements of the matrix must satisfy the following conditions [11]:

$$-s''_{11} > 0, \tag{A.6}$$

$$-s''_{33} > 0, \tag{A.7}$$

$$-s''_{44} > 0, \tag{A.8}$$

$$-s''_{11} \geqslant \left|-s''_{12}\right|, \tag{A.9}$$

$$s''_{11}s''_{33} \geqslant \left(s''_{12}\right)^2, \tag{A.10}$$

$$s''_{33}\left(s''_{11} + s''_{12}\right) \geqslant 2\left(-s''_{13}\right)^2, \tag{A.11}$$

where s_{ij} are the elements of the [S] matrix.

Using conditions (A.6) and (A.7) yields

$$Y'' > 0. \tag{A.12}$$

Using conditions (A.8)–(A.10) yield

$$\sigma' Y'' - \sigma'' Y' + Y'' \geqslant 0 \tag{A.13}$$

and

$$\sigma' Y'' - \sigma'' Y' - Y'' \leqslant 0. \tag{A.14}$$

Using condition (A.11) yields

$$2(\sigma' Y'' - \sigma'' Y')^2 - Y''(\sigma' Y'' - \sigma'' Y' + Y'') \leqslant 0. \tag{A.15}$$

Considering inequalities (A.13)–(A.15) simultaneously yields

$$-\frac{Y''(0.5-\sigma')}{Y'} \leqslant \sigma'' \leqslant \frac{Y''(1+\sigma')}{Y'}. \tag{A.16}$$

Finally, it is seen that all the conditions reduce to (A.12) and (A.16). The imaginary part of Young's modulus is always positive but the imaginary part of Poisson's ratio can be negative.

References

[1] D.D. Ebenezer, R. Ramesh, Analysis of axially polarized piezoelectric cylinders with arbitrary boundary conditions on flat surfaces, *Journal of the Acoustical Society of America* 113 (4) (2003) 1900–1908.

[2] D.D. Ebenezer, K. Ravichandran, C. Padmanabhan, Forced vibrations of solid elastic cylinders, *Journal of Sound and Vibration* 282 (2005) 991–1007.

[3] D.D. Ebenezer, K. Ravichandran, R. Ramesh, C. Padmanabhan, Forced responses of solid axially polarized piezoelectric ceramic finite cylinders with internal losses, *Journal of the Acoustical Society of America* 117 (6) (2005) 3645–3656.

[4] K.P. Soldatos, Review of three dimensional dynamic analyses of circular cylinders and cylindrical shells, *Applied Mechanics Reviews* 47 (10) (1994) 501–516.

[5] O.B. Wilson, *Introduction to the Theory and Design of Sonar Transducers Peninsula*, Los Altos, CA, USA, 1988.

[6] D. Stansfield, *Underwater Electroacoustic Transducers*, Bath University Press, UK, 1990.

[7] A. Iula, R. Carotenuto, M. Pappalardo, An approximated 3-D model of the Langevin transducer and its experimental validation, *Journal of the Acoustical Society of America* 111 (2002) 2675–2680.

[8] L. Shuyu, Analysis of the sandwich piezoelectric ultrasonic transducer in coupled vibration, *Journal of the Acoustical Society of America* 117 (2) (2005) 653–661.

[9] W.A. Smith, B.A. Auld, Modeling 1–3 composite piezoelectrics: thickness mode oscillations, *IEEE Transactions on Ultrasonics Ferrolectrics and Frequency Control* 38 (1991) 40–47.

[10] J.R. Hutchinson, Axisymmetric vibrations of a free finite length rod, *Journal of the Acoustical Society of America* 51 (1972) 233–240.

[11] R. Holland, Measurement of piezoelectric phase angles in a ferroelectric ceramic, *IEEE Transactions on Sonics Ultrasonics* SU-17 (2) (1970) 123–124.

[12] *ATILA Users Manual Version 5.2.4*. ISEN, Lilee Cedex, France.

[13] I.S. Sokolnikoff, *Mathematical Theory of Elasticity*, McGraw-Hill, New York, 1956.

[14] L. Cremer, M. Heckl, E.E. Ungar, *Structure-Borne Sound*, Springer, New York, USA, 1988 179pp.

[15] M. Abramowitz, I.A. Stegun (Eds.), *Handbook of Mathematical Functions*, Dover, New York, 1965 (Eqs. 11.3.20, 11.3.29, and 11.4.5).

[16] J.R. Hutchinson, Axisymmetric vibrations of a solid elastic cylinder encased in a rigid container, *Journal of the Acoustical Society of America* 51 (1967) 398–402.

[17] G.M.L. Gladwell, D.K. Vijay, Natural frequencies of free finite-length circular cylinders, *Journal of Sound and Vibration* 42 (3) (1975) 387–397.

[18] A.W. Leissa, J. So, Accurate vibration frequencies of circular cylinders from three-dimensional analysis, *Journal of the Acoustical Society of America* 98 (4) (1995) 2136–2141.

[19] A. Bayón, F. Gascón, F.J. Nieves, Estimation of dynamic elastic constants from the amplitude and velocity of Rayleigh waves, *Journal of the Acoustical Society of America* 117 (6) (2005) 3469–3477.